Article

One- and Two-Electron Oxidations of β-Amyloid$_{25\text{-}35}$ by Carbonate Radical Anion (CO$_3^{\bullet-}$) and Peroxymonocarbonate (HCO$_4^-$): Role of Sulfur in Radical Reactions and Peptide Aggregation

Antonio Francioso [1,2,*] 🄳, **Alessia Baseggio Conrado** [1,3] 🄳, **Carla Blarzino** [1], **Cesira Foppoli** [4], **Elita Montanari** [5], **Simone Dinarelli** [6], **Alessandra Giorgi** [1], **Luciana Mosca** [1,*] 🄳 and **Mario Fontana** [1,*] 🄳

[1] Department of Biochemical Sciences, "Sapienza" University of Rome, 00185 Rome, Italy; a.baseggioconrado@dundee.ac.uk (A.B.C.); carla.blarzino@uniroma1.it (C.B.); Alessandra.giorgi@uniroma1.it (A.G.)

[2] Departament of Organic Chemistry, Instituto Universitario de Bio-Orgánica "Antonio González", University of La Laguna, La Laguna, 38296 Tenerife, Spain

[3] Molecular and Clinical Medicine, University of Dundee, Ninewells Hospital and Medical School, Dundee DD1 9SY, UK

[4] Institute of Molecular Biology and Pathology, CNR National Research Council-Rome, 00185 Rome, Italy; Cesira.foppoli@uniroma1.it

[5] Department of Drug Chemistry and Technology, "Sapienza" University of Rome, 00185 Rome, Italy; Elita.montanari@uniroma1.it

[6] Institute for Structure of Matter, CNR National Research Council-Rome, 00133 Rome, Italy; simone.dinarelli@artov.ism.cnr.it

* Correspondence: antonio.francioso@uniroma1.it (A.F.); Luciana.mosca@uniroma1.it (L.M.); mario.fontana@uniroma1.it (M.F.)

check for updates

Abstract: The β-amyloid (Aβ) peptide plays a key role in the pathogenesis of Alzheimer's disease. The methionine (Met) residue at position 35 in Aβ C-terminal domain is critical for neurotoxicity, aggregation, and free radical formation initiated by the peptide. The role of Met in modulating toxicological properties of Aβ most likely involves an oxidative event at the sulfur atom. We therefore investigated the one- or two-electron oxidation of the Met residue of Aβ$_{25\text{-}35}$ fragment and the effect of such oxidation on the behavior of the peptide. Bicarbonate promotes two-electron oxidations mediated by hydrogen peroxide after generation of peroxymonocarbonate (HCO$_4^-$, PMC). The bicarbonate/carbon dioxide pair stimulates one-electron oxidations mediated by carbonate radical anion (CO$_3^{\bullet-}$). PMC efficiently oxidizes thioether sulfur of the Met residue to sulfoxide. Interestingly, such oxidation hampers the tendency of Aβ to aggregate. Conversely, CO$_3^{\bullet-}$ causes the one-electron oxidation of methionine residue to sulfur radical cation (MetS$^{\bullet+}$). The formation of this transient reactive intermediate during Aβ oxidation may play an important role in the process underlying amyloid neurotoxicity and free radical generation.

Keywords: peroxymonocarbonate; carbonate radical anion; β-amyloid; methionine sulfoxide; sulfur centered radical; reactive sulfur species; sulfur radical cation

1. Introduction

Alzheimer's disease (AD) is one of the most disabling dementia disorders among the elderly, characterized by progressive loss of memory and cognitive functions. Neurofibrillary tangles of

tau protein, neuronal loss, and amyloid plaques are the hallmarks of the disease [1,2]. The major constituent of the amyloid plaques is a 39–43 amino acid peptide named β-amyloid peptide (Aβ) which, through conformational modifications, becomes prone to form aggregates—from soluble oligomers or protofibrils to insoluble large fibrils—and is therefore responsible for various pathological effects [3,4]. Amyloid formation is generally associated with the AD clinical manifestations and there are many reports of Aβ peptides being toxic to neuronal cells [5–7]. Although the central role of Aβ in the pathogenesis of the disease is undisputed, the precise mechanism(s) of action and the nature of the toxic species remain to be identified [8].

The damage caused by oxidative stress may play an important role in the initiation and progression of AD. It has been shown that the AD brain is subject to increased oxidative stress [9,10] and that increased Aβ deposits are associated with the sites where neurodegeneration and oxidative stress coexist [11]. According to this, in the Aβ-associated oxidative stress model of neurodegeneration, the peptide is directly responsible for free radical-mediated damage to neuronal membrane systems, leading to subsequent neuronal loss [12–14]. Different studies have suggested that the toxic effects of Aβ involve its own oxidation and free radical generation, ascribing a critical role to the methionine (Met) residue at 35 position in the Aβ peptide [14–16]. Met-35 is one of the most susceptible residues to be oxidized [17], especially under oxidative stress conditions [18] and is essential for peptide neurotoxicity [19]. In fact, when it is replaced by norleucine or cysteine [19,20] or when it is sequestered within a lipid environment [21], or when it is lacking, as in Aβ$_{1-28}$, the peptide loses its neurotoxic properties.

In the oxidative event that occurs on Met-35 residue, the thioether sulfur can undergo a two- or one-electron oxidation (Scheme 1). The two-electron oxidation leads to the production of methionine sulfoxide (MetSO) [22], that could be further reduced to Met for the intervention of MetSO reductase, an enzyme whose activity is reduced in AD brains [23], or further oxidized to Met sulfone. Instead, the one-electron oxidation of the thioether sulfur leads to the formation of a positive charged sulfur radical (MetS$^{\bullet+}$) [24].
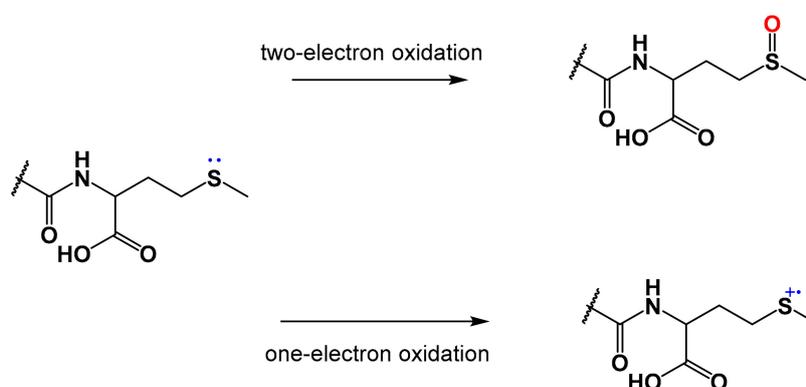
Scheme 1. One- and two-electron oxidations of Aβ$_{25-35}$ methionine residue on the thioether sulfur.

In order to better elucidate the biochemical process underlying amyloid neurotoxicity and free radical generation, we investigated the oxidative modifications of Aβ by two oxidants derived from the main physiological buffer, the bicarbonate/carbon dioxide pair: peroxymonocarbonate, HCO$_4^-$ (PMC), that catalyzes a two-electron oxidation, and carbonate radical anion (CO$_3^{\bullet-}$), which is a one-electron oxidant. The experiments were performed by using Aβ$_{25-35}$, a fragment of the full length peptide Aβ$_{1-42}$, containing 11 amino acids and presenting Met-35 as C-terminal residue, which has been shown to be more rapidly toxic and to cause more oxidative damage than the native full-length peptide [25]. Regarding the oxidant species, PMC was generated by the reaction of bicarbonate with hydrogen peroxide [26], while carbonate radical anion was generated by SOD/H$_2$O$_2$ system in the presence of bicarbonate [27,28]. Products derived from Aβ$_{25-35}$ oxidation were analyzed by HPLC and mass

spectrometry and the effects of such oxidation on the aggregation of the peptide were determined by means of spectrofluorimetry, atomic force microscopy, and dynamic light scattering.

2. Results

2.1. Oxidation of Aβ₂₅₋₃₅ Fragment by PMC (HCO_4^-)

The oxidation of Aβ$_{25-35}$ fragment by PMC was evaluated by HPLC. The chromatographic profiles of Aβ$_{25-35}$ solution were incubated for 120 min with HCO_4^- evidenced, in addition to the peak corresponding to the parent Aβ$_{25-35}$ fragment (Met-Aβ$_{25-35}$) at 15 min retention time (RT), the formation of a new peak (MetSO-Aβ$_{25-35}$) with a RT of 11 min (Figure 1).

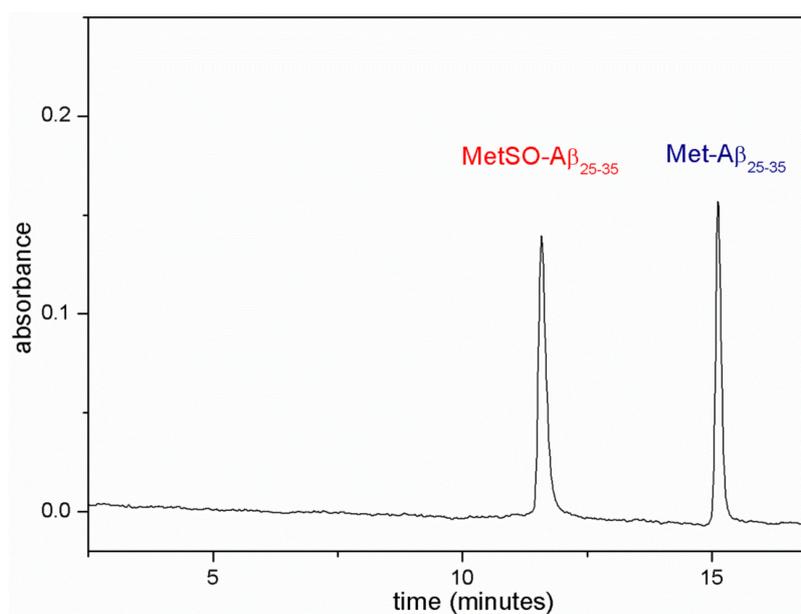**Figure 1.** HPLC profile of Aβ$_{25-35}$ incubated for 120 min with peroxymonocarbonate (PMC or HCO_4^-). 10 μM Aβ$_{25-35}$ was allowed to react with peroxymonocarbonate at 0.8 mM final concentration in 0.1 M phosphate buffer, pH 7.4, containing 0.1 mM DTPA. After 120 min at room temperature, aliquots of incubation mixture were analyzed by HPLC.

Taking into account that the only residue susceptible to be oxidized in the fragment is the Met located at 35 position [18] and the oxidative reactions mediated by PMC proceed through a bi-electronic mechanism [22], the production of the Aβ$_{25-35}$ fragment with the Met residue oxidized to methionine sulfoxide (MetSO-Aβ$_{25-35}$) is expected. In order to confirm this, eluted compounds from HPLC analysis corresponding to the two peaks were collected and analyzed by mass spectrometry. Mass spectra of the two fractions are shown in Figure 2. The two main molecular ions, at m/z = 1060 and 1076, correspond respectively to Aβ$_{25-35}$ and the same peptide with an additional oxygen atom, confirming the formation of MetSO residue.

The time-dependent conversion of Aβ$_{25-35}$ to MetSO-Aβ$_{25-35}$ by the bi-electronic oxidation was monitored by HPLC analysis. Figure 3 shows the concomitant Met-Aβ$_{25-35}$ diminution and MetSO-Aβ$_{25-35}$ increase.

MetSO-Aβ$_{25-35}$ formation was also evidenced by HPLC analysis when the peptide was incubated with hydrogen peroxide. The oxidation ability of hydrogen peroxide was lower than that of PMC. In fact, an amount of 41% of amyloid was found to be oxidized after 120 min incubation with PMC, while only 18% was oxidized after the same incubation time with hydrogen peroxide (Figure 4, left).

The sensitiveness to oxidation by HCO_4^- of the Met residue in the Aβ$_{25-35}$ peptide was compared to that of free L-Met in the same experimental conditions. Figure 4 (right) shows that the free amino acid was oxidized to a higher extent compared to the Met residue of the peptide.
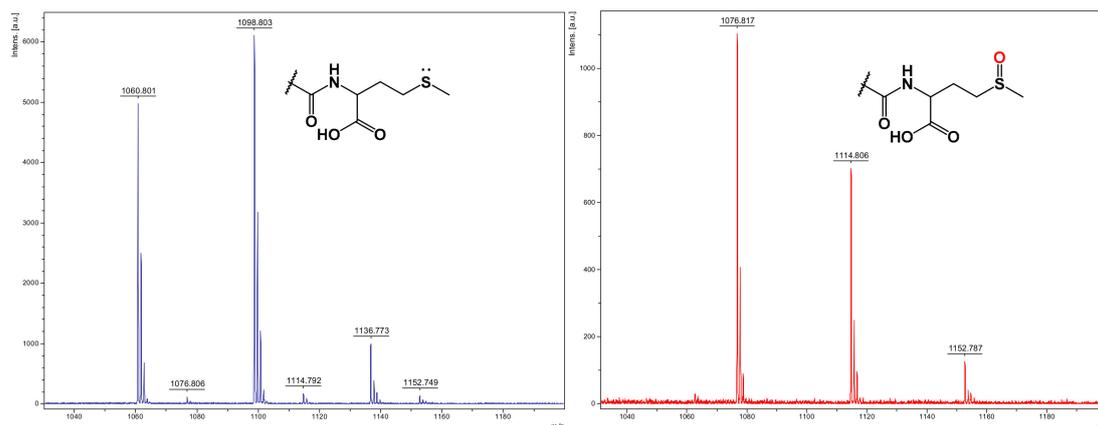
Figure 2. Mass spectra (*m/z*) obtained by MALDI-ToF MS analysis related to Aβ$_{25-35}$ (**left**) and the same peptide with the methionine residue oxidized to methionine sulfoxide (**right**). 1060 and 1076 *m/z* correspond to Met-Aβ$_{25-35}$ and MetSO-Aβ$_{25-35}$, respectively. The peaks at 1098, 1136, 1114, and 1152 *m/z* are related to their +K [M + 39] and +2K [M + 76] *m/z* adducts.
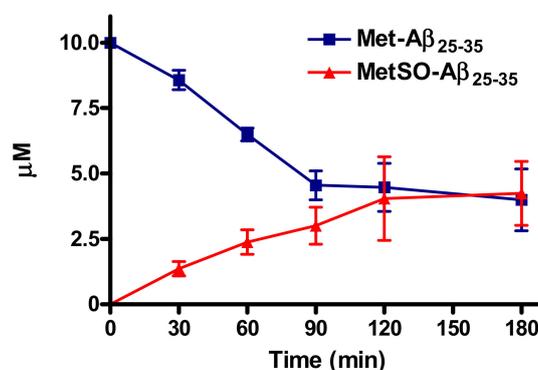

Figure 3. Time course of Aβ$_{25-35}$ oxidation by peroxymonocarbonate. To a reaction mixture containing 10 μM Aβ$_{25-35}$ in 0.1 M phosphate buffer, pH 7.4, and 0.1 mM DTPA, peroxymonocarbonate was added at 0.8 mM final concentration. At various time intervals of incubation at 37 °C, the reaction was stopped by addition of catalase (400 U/mL) and the reaction products were analyzed by HPLC.
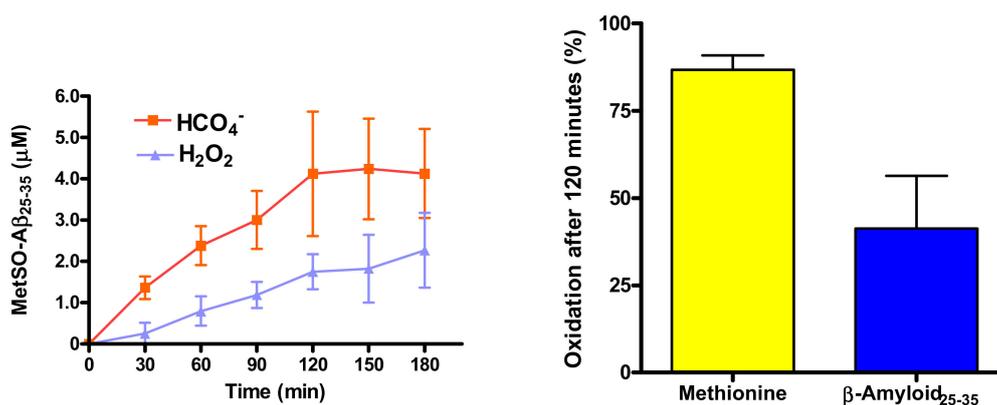

Figure 4. Time course of Aβ$_{25-35}$ oxidation by peroxymonocarbonate or hydrogen peroxide (**left**). Aβ$_{25-35}$ and L-methionine oxidation by peroxymonocarbonate at 120 min (**right**). To reaction mixture containing 10 μM Aβ$_{25-35}$ or 10 μM L-methionine in 0.1 M phosphate buffer, pH 7.4, and 0.1 mM DTPA, peroxymonocarbonate was added at 0.8 mM final concentration. Hydrogen peroxide was 5 mM. At various time intervals of incubation at 37 °C, the reaction was stopped by addition of catalase (400 U/mL) and the reaction products analyzed by HPLC.

2.2. Oxidation of Free Methionine and Aβ25-35 by $CO_3^{\bullet-}$ (SOD/H2O2/Bicarbonate System)

Oxidative reactions mediated by SOD/H$_2$O$_2$ system in the presence of bicarbonate proceeded through a mono-electronic mechanism by which the highly reactive carbonate radical anion ($CO_3^{\bullet-}$) is formed. The effect of HCO$_3^-$/CO$_2$ pair on the oxidation of free L-Met in the presence of SOD/H$_2$O$_2$ was indirectly evaluated quantifying the production of MetSO by HPLC. As shown in Figure 5, free Met was almost completely consumed after 60 min incubation in the presence of SOD/H$_2$O$_2$/bicarbonate system. However, only a fraction (about 50%) was transformed in MetSO. It can be rationally assumed that the remaining part was oxidized by $CO_3^{\bullet-}$ through a mono-electronic mechanism to its radical cation form (MetS$^{\bullet+}$), and then degraded to volatile sub-products, such as ammonia, carbon dioxide, and methanthiol, undetectable by HPLC analysis [29–31].
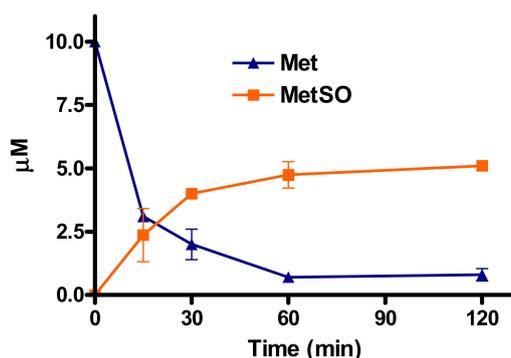

Figure 5. Oxidation of free L-methionine by carbonate radical anion. 10 μM L-methionine was incubated at 37 °C with 31 μM SOD, 25 mM sodium bicarbonate, 0.1 mM DTPA in 0.1 M phosphate buffer, pH 7.4. Reaction was started by the addition of 1 mM H$_2$O$_2$. At various time intervals, the reaction was stopped by addition of catalase (400 U/mL) and the reaction products analyzed by HPLC.

On the other hand, in the absence of HCO$_3^-$/CO$_2$, the SOD/H$_2$O$_2$ system determined the full oxidation of L-Met to its sulfoxide. This can be explained by the fact that in these conditions the reaction of SOD with hydrogen peroxide generates $^{\bullet}$OH radical that inactivates the enzyme [32]; therefore, the observed oxidation was due exclusively to a two-electron mechanism mediated by H$_2$O$_2$ excess (not shown).

When the Aβ25-35 was incubated with the SOD/H$_2$O$_2$/bicarbonate system under the same experimental conditions, the peak corresponding to the peptide completely disappeared in HPLC chromatogram, but no new peak appeared.

Therefore, the evaluation of one-electron Aβ25-35 oxidation was indirectly performed by determining the rate of dihydrorhodamine-123 (DHR) oxidation through mono-electronic mechanism (Scheme 2).
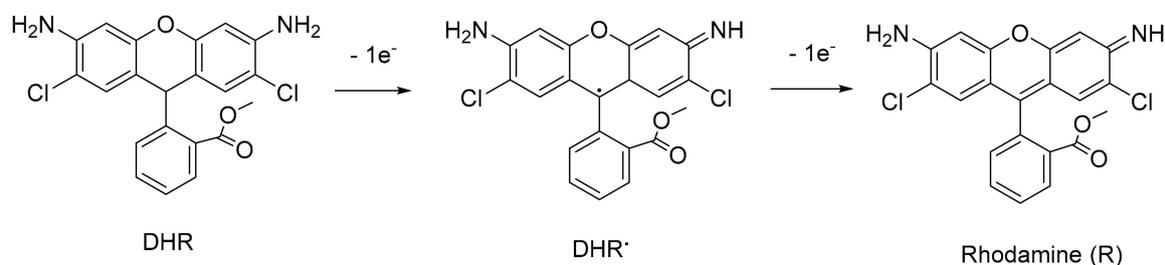
Scheme 2. Two-step mono-electronic oxidation of dihydrorhodamine-123 (DHR).

In the presence of $CO_3^{\bullet-}$, DHR is oxidized first to DHR$^{\bullet}$ radical, and subsequently another electron is abstracted to produce fully oxidized rhodamine (R):

$$DHR + CO_3^{\bullet-} \rightarrow DHR^{\bullet} + CO_3^{2-}$$

$$DHR^\bullet + CO_3^{\bullet-} \rightarrow R + CO_3^{2-}$$
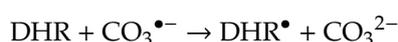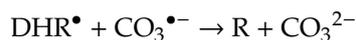
Interestingly, $A\beta_{25\text{-}35}$ acts as a "scavenger", competing with DHR in the reaction with carbonate radical anion generated by the SOD/H_2O_2/bicarbonate system and showed a much higher ability than free Met in inhibiting the carbonate radical anion-mediated DHR oxidation (Figure 6). The scavenging activity of the free amino acid was very low and a 100-fold Met concentration higher than that of peptide was required to obtain a similar reduction of DHR oxidation rate (not shown).
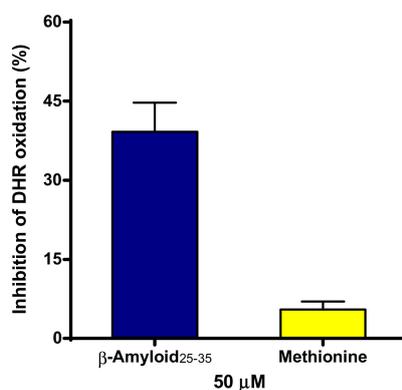

Figure 6. Effect of $A\beta_{25\text{-}35}$ and L-Met on DHR oxidation mediated by carbonate radical anion. $A\beta_{25\text{-}35}$ or L-methionine (50 μM final concentration) was added to a solution containing 25 μM DHR, 31 μM SOD, 0.1 mM DTPA, and 25 mM sodium bicarbonate in 0.2 M phosphate buffer, pH 7.4. Reaction was started by the addition of 1 mM H_2O_2. Oxidized DHR was quantified spectrophotometrically at 500 nm.

Noteworthily, the ability of the amyloid to protect DHR from oxidation is exclusive for the non-aggregated peptide. When $A\beta_{25\text{-}35}$ was incubated for longer times in DTPA and phosphate buffer (aggregation-favoring conditions), it failed to protect DHR from one-electron oxidation by $CO_3^{\bullet-}$. Rather, the oxidation rate of DHR in the presence of aggregated peptide was even enhanced compared to the control. Figure 7 shows the kinetics of DHR oxidation in the presence of two different states of $A\beta_{25\text{-}35}$ aggregation. After 24 h, during which the peptide was allowed to stay in aggregating conditions, the oxidation rate of DHR was 1.3 fold higher than that of control. The same behavior with lower radical scavenging effects on reaction kinetics was observed using ABTS as a reagent instead of DHR by monitoring the formation of $ABTS^{+\bullet}$ radical cation (not shown).
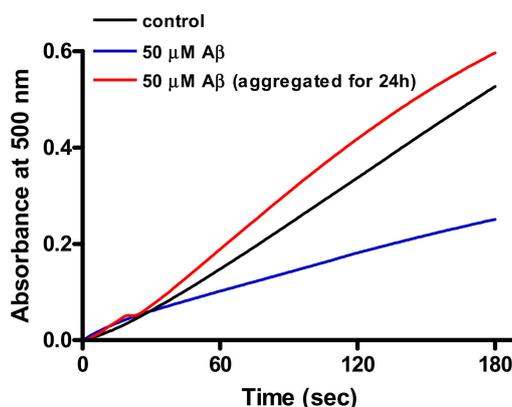

Figure 7. Effect of different aggregation states on the reaction rate of DHR oxidation by $CO_3^{\bullet-}$. Freshly dissolved $A\beta_{25\text{-}35}$ (blue line) and aggregated $A\beta_{25\text{-}35}$ (red line) after 24 h incubation. $A\beta_{25\text{-}35}$ (50 μM final concentration) was added to a solution containing 25 μM DHR, 31 μM SOD, 0.1 mM DTPA, and 25 mM sodium bicarbonate in 0.2 M phosphate buffer, pH 7.4. Reaction was started by the addition of 1 mM H_2O_2. DHR oxidation rate was measured spectrophotometrically at 500 nm.

2.3. Effect of One-Electron and Two-Electron Oxidation on Aβ25-35 Aggregation

The effect of the two different oxidative modifications of Aβ25-35 exerted by HCO_4^- or $CO_3^{\bullet-}$ on Aβ25-35 aggregation were investigated by means of spectrofluorimetry (Thioflavin-T assay), dynamic light scattering (DLS), and atomic force microscopy (AFM).

A major consideration needs to be taken into account while using AFM to assess the structures of Aβ samples prepared with the drop casting method on mica: although this deposition technique is quite common and easy to apply, it confers a high heterogeneity to the sample, hampering a quantitative statistical analysis of the observed structures [33]. However, the high resolution of the technique can provide, under some circumstances, a clear idea of the sample properties, i.e., it can be clearly observed whether there are substantial differences among the samples [33]. Figure 8 reports typical images of the specimens, which clearly present morphological differences. As shown in panel (a) in the blank sample there are huge amorphous aggregates of several microns in size and many structures in the order of several hundreds of nanometers that look globular. Panel (b) reports the typical landscape of the one-electron oxidation sample that appears similar to the previous one in terms of co-presence of big aggregates and smaller globular structures. In this case, however, the presence of aggregates of several microns of diameter is reduced and the globular structures ranges from one to some hundreds of nanometers. From an atomic microscopic point of view, this sample looks similar to the previous aggregated Aβ25-35 but observed one step before that the huge aggregation process takes place. Finally, in panel (c) of Figure 8, a representative image of the two-electron oxidation sample is shown. In this case the topography is dramatically different, the sample appears scattered, and none of the huge aggregates discussed above have been found, more precisely no structures with diameter of one micron were found. This sample is mainly constituted of small elongated structure of the nanometer range in length, that resemble the fibrillary structure of amyloid fibrils maybe at the very first steps of the aggregation process. It should be noticed that one single fibril per field of view was imaged.
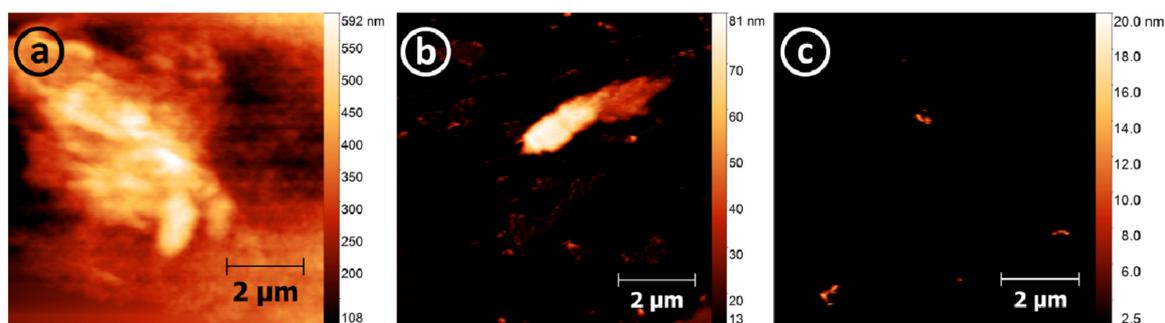

Figure 8. Atomic force microscopy (AFM) typical morphologies of aggregated Aβ25-35 in the presence or absence of HCO_4^- (two-electron oxidant) or $CO_3^{\bullet-}$ (one-electron oxidant) after 24 h aggregation. The aggregated amyloid (**a**) sample present almost everywhere amorphous structures and globular aggregates of several microns in size. The one-electron reaction (**b**) sample is similar to the aggregated one in terms of dimensions of the aggregates but their presence is diminished. Two-electron oxidation sample (**c**), instead, present smaller and scattered structures of elongated nature, in this latter sample very rarely were observed amorphous structures of several hundreds of nanometers in size.

Thioflavin-T (Th-T) assay revealed that after 24 h incubation (Figure 9) the one-electron oxidation mediated by $CO_3^{\bullet-}$ inhibits peptide aggregation for a 10% with respect to the control aggregated Aβ25-35. On the other hand, the PMC oxidation of thioether sulfur to sulfoxide (HCO_4^--mediated two-electron oxidation) induces less than 40% aggregation compared to the fully aggregated peptide.

The time-dependent aggregation on HCO_4^- oxidized peptide was also investigated by HPLC. The aggregated amyloid peptide was indirectly quantified by determining the decrease of soluble amyloid peptide. As confirmed by HPLC (Figure 10), the amount of aggregated peptide formed in the

presence of HCO_4^- was lower compared to that formed in the absence of the oxidant. A decrease of about 40% was observed after 180 min incubation with PMC.
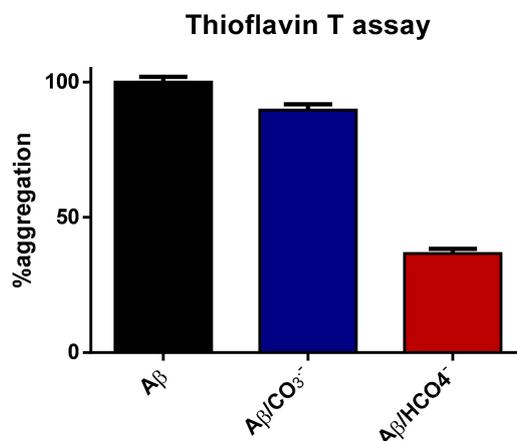
Thioflavin T assay

Figure 9. Thioflavin-T fluorimetric aggregation assay of $A\beta_{25-35}$ in the presence or absence of HCO_4^- (two-electron oxidant) or $CO_3^{\bullet-}$ (one-electron oxidant) after 24 h aggregation.
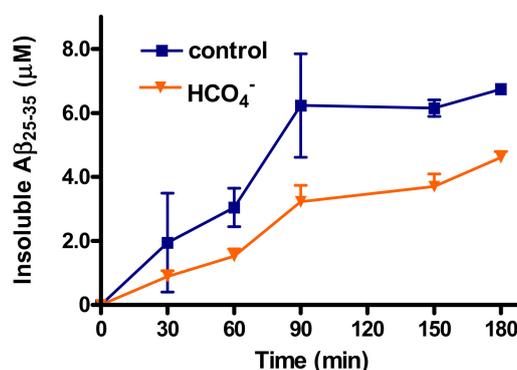

Figure 10. $A\beta_{25-35}$ aggregation in the presence or absence of peroxymonocarbonate. Reaction mixture contained 10 μM $A\beta_{25-35}$ in 0.1 M phosphate buffer, pH 7.4, and 0.1 mM DTPA (squares), when present, peroxymonocarbonate was added at 0.8 mM final concentration (triangles). After various time incubation at 37 °C, the reaction was stopped by addition of catalase (400 U/mL) and the reaction products analyzed by HPLC.

The effect on aggregation and on the tendency of the oxidized peptide to aggregate was explored also by dynamic light scattering experiments. The same samples for AFM and Thioflavin-T analyses were analyzed by DLS after filtering samples through 0.45 μm pore diameters filters. As shown in Figure 11, control $A\beta_{25-35}$ and $CO_3^{\bullet-}$-exposed $A\beta_{25-35}$ (one-electron oxidation) revealed the presence of aggregated particles with micron-scale diameter while the two-electron oxidation of $A\beta_{25-35}$ stops its tendency to form aggregates, maintaining the smaller nano-scale formed particles.
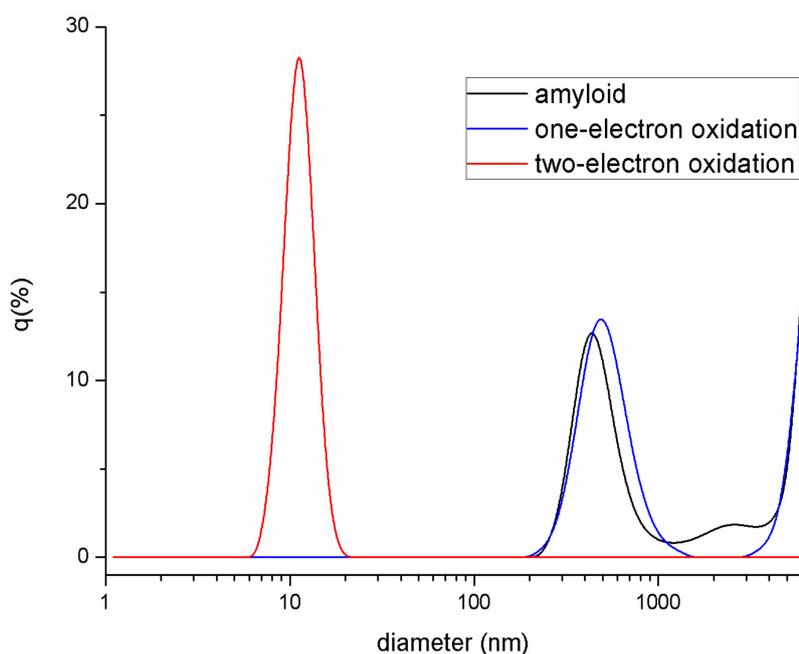
Figure 11. Dynamic light scattering (DLS) analyses of $A\beta_{25-35}$ in the presence or absence of HCO_4^- (two-electron oxidant) or $CO_3^{\bullet-}$ (one-electron oxidant). Only the sulfoxide formation (red line) mediated by HCO_4^- stops the aggregation process at nano-scale level.

3. Discussion

Oxidative damage and amyloid accumulation are the key factors in the pathogenesis of AD. The mechanism by which the amyloid peptide exerts its toxicity is still unknown, but an association between Aβ toxicity and oxidative stress has been suggested and confirmed by several studies [34–36].

The Aβ fragment used in this work, the $A\beta_{25-35}$, retains the toxic and aggregation properties of the full-length peptide $A\beta_{1-42}$ [6,25], which is the most abundant form in senile plaques. Indeed, $A\beta_{25-35}$ contains the Met-35 residue that, being the main target of oxidative reactions, is thought to be responsible for the Aβ ability to generate free radicals and oxidative stress.

In this work we show that $A\beta_{25-35}$ undergoes oxidative modifications by the action of oxidants derived from the buffer HCO_3^-/CO_2, i.e., PMC and carbonate radical anion. Indeed, a role of the main physiological buffer in modulating biological oxidations is well established [37–39]. Even if both PMC and carbonate radical anion derive from the same system, the reactions mediated by the two oxidants proceed through different mechanisms: HCO_4^- is prevalently a two-electron oxidant, while $CO_3^{\bullet-}$ is responsible for one-electron oxidations.

PMC can be generated through the equilibrium between bicarbonate and H_2O_2 and is capable of oxidizing a variety of organic compounds. Owing to the fact that bicarbonate concentration in tissues under physiological conditions is high (≥25 mM) and, for a fixed hydrogen peroxide concentration, the rate of PMC formation is likely to be similar to that expected for hydroxyl radical formation from redox-active iron(II) [40,41], HCO_4^- can be considered an reliable biological oxidant.

Our results indicate that PMC is able to oxidize thioether sulfur of Met-35 residue of $A\beta_{25-35}$ to sulfoxide (MetSO). The Met oxidation to MetSO is well known and its presence in proteins is an established marker of oxidative stress [18,42,43]. Mechanisms of oxidation of sulfides and free methionine by PMC have been widely studied by Richardson and co-workers [44,45]. We observed that PMC is more potent than hydrogen peroxide as concerns the Aβ oxidation, in accordance with some experimental evidence on the ability of the bicarbonate/carbon dioxide system to promote oxidation, peroxidation and nitration of several biological targets in the presence of hydrogen peroxide [37,46]. In these conditions, PMC is considered the chemical species responsible for the increment of oxidative reactions. Although the formation of HCO_4^- from hydrogen peroxide and bicarbonate in aqueous
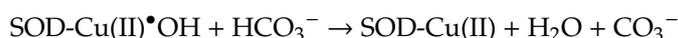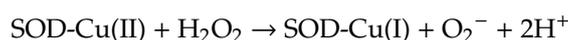
solution at neutral pH is a relatively low process (k = 10^{-2} $M^{-1}sec^{-1}$), this value is influenced by the presence of proteins and lipids [40], indicating that PMC can be physiologically generated from hydrogen peroxide at high speed in biological tissues rich in proteins, lipids, and bicarbonate/CO_2.

Interestingly, our experiments show that Aβ_{25-35} two-electron oxidation counteracts the tendency of peptide to aggregate. This is in accordance with previous reports, indicating that the oxidation of Met-35 also alters the physical properties of the peptide, such as aggregation tendency, leading to a different oligomerization profile with significant attenuation of trimers and tetramers formation [47] and reduction of fibril assembly [48]. Additionally, recent molecular dynamics simulation experiments of Brown et al. [49] are consistent with a decrease in aggregation rate when Met-35 of Aβ_{1-40} is oxidized to sulfoxide. Moreover, it has been observed that Met oxidation of Aβ generates very different fiber morphologies compared to un-oxidized Aβ, with much shorter (<500 nm) fragmented fibers [50]. Noteworthily, also the inhibition of fibrillation of α-synuclein is mediated by methionine oxidation. It has been suggested that α-synuclein completely oxidized to its Met residues shows a reduced propensity to form amyloid fibrils, probably related to the interference of MetSO residues in oxidized protein to form ordered β-type secondary structures [51].

The fact that oxidized amyloid possesses attenuated aggregating capacity validates the hypothesis that oxidative stress in AD brain likely induces toxicity in a manner independent from fibril formation. This theory is also supported, considering the outcomes of the one-electron oxidation of Aβ_{25-35} by carbonate anion radical ($CO_3^{\bullet-}$). This strong oxidant acts by both electron transfer and hydrogen abstraction mechanisms to produce radicals from the oxidized targets [39] and is able to oxidize a broad series of compounds of biochemical interest [52], including sulfur amino acids of proteins [53] in which it adds to the sulfur atom, according to reactions [54]:

$$MetS + CO_3^- \rightarrow MetS^\bullet CO_3^-$$

$$MetS^\bullet CO_3^- \rightarrow MetS^+ + CO_3^{2-}$$
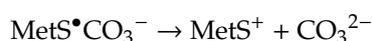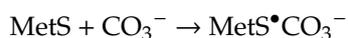
In our study $CO_3^{\bullet-}$ has been generated by SOD/H_2O_2/HCO_3^- system. Bicarbonate anion, owing its small size, can easily reach SOD active site, where is oxidized to $CO_3^{\bullet-}$ by hydroxyl radical ($^\bullet OH$) generated by the enzyme in the presence of hydrogen peroxide:

$$SOD\text{-}Cu(II) + H_2O_2 \rightarrow SOD\text{-}Cu(I) + O_2^- + 2H^+$$

$$SOD\text{-}Cu(I) + H_2O_2 \rightarrow SOD\text{-}Cu(II)^\bullet OH + OH^-$$

$$SOD\text{-}Cu(II)^\bullet OH + HCO_3^- \rightarrow SOD\text{-}Cu(II) + H_2O + CO_3^-$$

To investigate the susceptibility of Aβ_{25-35} fragment to mono-electronic oxidation by carbonate anion radical, we carried experiments using dihydrorhodamine-123 as a target of oxidative reaction by $CO_3^{\bullet-}$. We observed that the presence of Aβ_{25-35} determined a net decrease of DHR oxidation rate, due to the fact that the peptide competes with DHR for the $CO_3^{\bullet-}$. Instead, if Aβ_{25-35} is preventively incubated for long times in favoring aggregation conditions, the DHR oxidation rate results also 1.3 fold higher than that in absence of peptide. Therefore, the reactivity of amyloid with carbonate radical anion confers to the peptide an antioxidant effect until it is in unaggregated form. On the contrary, under conditions that favor the peptide aggregation, the antioxidant capacity is lost and the peptide becomes pro-oxidant. This behavior suggests the formation of radical intermediates able to promote the oxidative processes.

Compared to free methionine, Aβ_{25-35} was much more efficient as competitor of DHR for the $CO_3^{\bullet-}$-mediated oxidation (Figure 7). The low scavenger activity of free methionine is in accordance with previous reports [52] on the greater susceptibility of amino acid residues into proteins respect to free amino acids to be oxidized by carbonate anion radical. Additionally, our HPLC determinations showed that, when free methionine was allowed to react in the presence of SOD/H_2O_2/HCO_3^-,

it was only partially oxidized through one-electron transfer, and that a fraction was transformed in sulfoxide through two-electron oxidation; on the contrary, $CO_3^{\bullet-}$ completely oxidized $A\beta_{25-35}$, as demonstrated by the fact that in the same conditions no peak attributable to two-electron oxidation of Met residue appeared.

The pro-oxidant effect of $A\beta$ has been often correlated to its ability to chelate metals, copper above all, due to the presence of three histidine residues in the peptide chain [55,56] and it has been suggested that this ability could explain the presence of elevated concentration of copper and other transition metals in the senile plaques of AD subjects [57]. However, in our experiments, the pro-oxidant effect has been observed despite the presence of DTPA, a strong metal-chelating agent, and even though the truncated peptide we used, $A\beta_{25-35}$, lacks of metal-binding residues of native peptide $A\beta_{1-42}$. It can be therefore hypothesized that the observed pro-oxidant activity could be linked to the high reactivity of Met-35. Indeed, reactivity of methionine residues toward carbonate radical anion is in the order of 10^7 $M^{-1}sec^{-1}$, at least 100 fold greater than that of not-sulfur amino acids [52].

In the presence of $CO_3^{\bullet-}$, methionine residue undergoes one-electron oxidation, generating a sulfur radical cation. This "sulfur centered" radical is potentially pro-oxidant, since is able to remove hydrogen atoms from protein and lipids, causing protein oxidation and lipid peroxidation [58]. At pH 7.4, the C-terminal of $A\beta_{25-35}$, corresponding to methionine residue, is in the form of carboxylate anion. The negatively charged oxygen could favor the oxidation of thioether sulfur and the stabilization of the derived cation radical. Moreover, the $MetS^{\bullet+}$ radical cation in the full-length peptide $A\beta_{1-42}$ can be stabilized through bond formation with either the oxygen or the nitrogen atoms of adjacent peptide bond [59]. Likely, this radical remains stabilized also during the aggregation process, therefore making the peptide able to trigger oxidative reactions.

4. Materials and Methods

4.1. Reagents and Chemicals

$A\beta_{25-35}$ fragment (NH_2- and COOH-terminal free peptide), superoxide dismutase (SOD) from bovine erythrocytes (EC 1.15.1.1), catalase, diethylenetriaminepentaacetic acid (DTPA), and Thioflavin-T were obtained from Sigma (St. Louis, MO, USA). L-methionine and hydrogen peroxide (30%) were purchased from Fluka (Buchs, Switzerland). All other chemicals were of the highest purity commercially available. H_2O_2 concentration was verified using UV absorption at 240 nm ($\varepsilon = 43.6$ $M^{-1}cm^{-1}$) [60]. All solutions and buffers were prepared with distilled water purified in a Millipore (Burlington, MA, USA) Milli-Q system and contained DTPA to avoid metal-dependent oxidative reactions.

4.2. Synthesis of PMC (HCO_4^-)

0.9 mL of 0.5 M sodium bicarbonate were added to 0.1 mL of 0.5 M hydrogen peroxide and the solution was left to equilibrate at room temperature for 10 min. In these conditions, the concentration of formed HCO_4^- calculated by the equation: $[HCO_4^-] = 0.31 \times [H_2O_2] [HCO_3^-]$, where 0.31 is the value of k of equilibrium for the HCO_4^- formation [39], results to be 7.75 mM.

4.3. Two-Electron Oxidation of $A\beta_{25-35}$ Fragment and L-Methionine by PMC

To reaction mixture containing 10 μM $A\beta_{25-35}$ or 10 μM L-methionine in 0.1 M phosphate buffer, pH 7.4, and 0.1 mM DTPA, PMC was added at 0.8 mM final concentration. After incubation at 37 °C for various times, the reaction was stopped by addition of catalase (400 U/mL) and the reaction products were analyzed by HPLC and mass spectrometry (Waters, Milford, MA, USA; Bruker Daltonics, Bremen, Germany).

4.4. One-Electron Oxidation of $A\beta_{25-35}$ Fragment and L-Methionine by SOD/H_2O_2 System

To reaction mixture containing 10 μM $A\beta_{25-35}$ or 10 μM L-methionine in 0.1 M phosphate buffer, pH 7.4, and 0.1 mM DTPA, SOD was added at 31 μM final concentration, in the presence or absence

of 25 mM NaHCO$_3$. The reaction was started by the addition of hydrogen peroxide at 1 mM final concentration. After incubation at 37 °C for various times, the reaction was stopped by addition of catalase (400 U/mL) and the reaction products were analyzed by HPLC.

4.5. HPLC Analysis

HPLC analysis of methionine and methionine sulfoxide (Met-SO), the two-electron oxidation product, was performed with a Waters–Millipore Chromatograph (Milford, MA, USA) equipped with a model 600 pump, a model 600 gradient controller, and a Waters 474 scanning fluorescence detector (Milford, MA, USA). Samples were derivatized with *o*-phthalaldehyde-2-mercaptoethanol (OPA) prior to injection [61] and applied on a Symmetry C18 column (5μ, 4.6 mm × 250 mm). Elution was performed using as mobile phases: A) 50 mM sodium acetate buffer, pH 5.5-methanol (80:20, *v/v*) B) 50 mM sodium acetate buffer, pH 5.5-methanol (20:80, *v/v*), flow rate 1mL/min, at room temperature. The elution gradient was linear, from 100% A to 100% B in 30 min. The fluorescence of eluates was monitored at 340 nm (λ_{ex}) and 450 nm (λ_{em}). The retention time of L-methionine was 21 min and concentrations were calculated from a standard curve.

For analysis of Aβ$_{25-35}$ and its two-electron oxidation product, the UV Waters photodiode array detector was used. The chromatography was carried out on a Nova-Pak C18 column (4 μ, 3.9 mm × 150 mm). Elution was performed using as mobile phases: (A) 50 mM sodium phosphate buffer, pH 3.0-acetonitrile (90:10, *v/v*) (B) acetonitrile-water (50:50, *v/v*), flow rate 1mL/min, at room temperature and with a linear gradient from 100% A to 100% B in 30 min. The absorbance of eluates was monitored at 214 nm. The retention time of Aβ$_{25-35}$ was 15 min and its concentration was calculated from a standard curve using the Millenium 32 software (Waters). The same curve was used to determine oxidized Aβ$_{25-35}$ concentration, assuming the same absorbance at 214 nm for either Aβ$_{25-35}$ and its oxidized form.

4.6. Purification of the Product of Two-Electron Oxidation of Aβ$_{25-35}$ Fragment by PMC

Then, 10. μM Aβ$_{25-35}$ was allowed to react with PMC at 0.8 mM final concentration in 0.1 M phosphate buffer, pH 7.4, containing 0.1 mM DTPA. After 120 min at room temperature, aliquots of incubation mixture were loaded on Nova-Pak C18 column and subjected to HPLC in the conditions previously described. The eluates, monitored at 214 nm, corresponding to the product of two-electron oxidation of Aβ$_{25-35}$, with a retention time of 11 min, were collected and analyzed by MALDI-ToF MS spectrometry (Bruker Daltonics, Bremen, Germany) [62].

4.7. Mass Spectrometry

The peptide mixtures were loaded directly onto an appropriate MALDI target plate with 1 μL of α-cyano-4-hydroxy-trans-cinnamic acid matrix solution (10 mg/mL) in 70% acetonitrile containing 0.1% TFA (*v/v*). MALDI-ToF MS analyses were performed by an AutoFlex II (Bruker Daltonics, Bremen, Germany) equipped with a 337 nm nitrogen laser and operating in reflector mode. Mass data were obtained by accumulating several spectra from laser shots with an accelerating voltage of 20 kV.

4.8. Effect of L-Methionine and Aβ$_{25-35}$ Fragment on Dihydrorhodamine-123 (DHR)

Stock solution of 5 mM DHR in acetonitrile was prepared and stored in the dark at −20 °C. Appropriate aliquots of L-methionine or Aβ$_{25-35}$ (50 μM final concentration) were added to a solution containing 25 μM DHR, 31 μM SOD, 0.1 mM DTPA, and 25 mM sodium bicarbonate in 0.2 M phosphate buffer, pH 7.4. Reaction was started by the addition of 1 mM H$_2$O$_2$. Oxidized DHR was quantified spectrophotometrically at 500 nm (ε = 78,000 M^{-1}cm^{-1}) [63] with a UV-Vis Perkin-Elmer (Waltham, MA, USA).

4.9. Thioflavin-T (ThT), Atomic Force Microscopy (AFM), and Dynamic Light Scattering Analyses (DLS)

One-electron oxidation, two-electron oxidation, and control $A\beta_{25-35}$ (in PBS buffer) samples were incubated for 24 h at room temperature. An aliquot of each sample was used for ThT, AFM, and DLS experiments. Thioflavin T (ThT) binding assay was performed as reported [64]. Then, 50 μL of each sample was added to a fresh 5 μM solution of Thioflavin-T (dissolved in 50 mM glycine solution, pH 8.5) to rich a final 10 μM $A\beta_{25-35}$ concentration. Fuorescence was measured on a SPEX-Fluoromax spectrofluorometer (Horiba Scientific, Horiba Ltd., Kyoto, Japan) with λ_{ex} = 440 nm and λ_{em} = 485 nm. The results are presented as mean and S.D. of three separate measurements.

The samples for the AFM characterization were prepared by the casting method, by manually dropping 5 μL of sample solution onto freshly cleaved mica and then air dried overnight, as previously described [33]. The AFM images were acquired using a home-designed microscope, described in detail elsewhere [65], operating in contact mode, in air, at room temperature and constant 30% relative humidity. The AFM tips chosen were made of silicon nitride (Veeco, New York, NY, USA) with tip of asymmetric pyramidal shape and nominal radius on 10 nm. During the imaging the vertical force was maintained below 1 nN in order to not damage the samples. The acquired images (8 × 8 micron, 600 × 600 points) were then treated using the freeware software Gwyddion (www.gwyddion.net).

For DLS experiments each samples was filtered onto 0.45 μm filters to retain insoluble and over micron scale aggregates and analyzed after one hour from filtration. The DLS measurements were taken using a HORIBA LB-550 instrument at a 650 nm Laser diode wavelength (5 mW), with a temperature control capacity set at 25 °C. To ensure accurate readings, the final distribution was taken from an accumulation of 100 individual DLS collections of three individual aliquots for each sample.

4.10. Statistics

Results are expressed as means ± SEM for at least three separate experiments performed in duplicate. Graphics and data analysis were performed using GraphPad Prism 4 software.

5. Conclusions

Although the origin of oxidative damage in AD is not yet fully understood, our experiments confirm that amyloid peptide is liable to be oxidized at level of methionine residue and that the effects of such oxidation vary depending whether one- or two-electron mechanisms are implied. While bi-electronic oxidation of the thioether sulfur of Met-35 to sulfoxide determines an attenuation of aggregation capacity of the peptide, as demonstrated by our and other authors' experiments [19], the one-electron oxidation leads to the formation of sulfur radical cation $(MetS^{\bullet+})$. The latter, like other radicals with sulfur in high oxidation states that can be originated in vivo in oxidative stress conditions [66], has oxidizing properties similar to ROS and is able to trigger and spread oxidative reactions. Therefore, though the sulfur-containing biomolecules have antioxidant activity, the transient formation of these reactive species during redox reactions may have a patho-physiological relevance [67]. This is a further confirmation of the model of free radical-based neurotoxicity of Aβ in AD, supported by numerous lines of evidence [16,24], according which the peptide initiates free radical processes resulting in protein oxidation, lipid peroxidation, reactive oxygen species formation, and cellular dysfunctions leading to neuronal death [16].

Finally, it is noteworthy that the oxidative agents used in this work, i.e., PMC and carbonate radical anion, derive in vivo from the main physiological buffer, the bicarbonate/CO_2 pair, which can promote either mono-electronic oxidations mediated by peroxynitrite, SOD, xanthine oxidase, or bi-electronic oxidations mediated by hydrogen peroxide. The high bicarbonate concentration physiologically present in tissues makes the importance of the two species very considerable. The described processes may occur in physiological conditions, and the inclusion of these species within the more prominent biological oxidants can give new prompts in the comprehension and control of the mechanisms of many pathologies.

It should be emphasized that free radicals and oxidants are currently considered as important mediators in the response of various signaling molecules and pathways involved in physiologic and pathologic processes. A better understanding of cellular oxidative mechanisms, many of which are likely to be modulated by the ubiquitous bicarbonate/carbon dioxide pair, can be very helpful for the elucidation of these interrelated processes.

Abbreviations

Aβ	β-amyloid
AD	Alzheimer's disease
DTPA	diethylenetriaminepentaacetic acid
DHR	dihydrorodhamine-123
MetSO	methionine sulfoxide
MetS$^{\bullet+}$	methionine sulfur radical cation
PMC	peroxymonocarbonate (HCO_4^-)

References

1. Braak, H.; Braak, E. Neuropathological stageing of Alzheimer-related changes. *Acta Neuropathol.* **1991**, *82*, 239–259. [CrossRef]

2. Selkoe, D.J. Soluble oligomers of the amyloid β-protein impair synaptic plasticity and behavior. *Behav. Brain Res.* **2008**, *192*, 106–113. [CrossRef]

3. Hartley, D.M.; Walsh, D.M.; Ye, C.P.; Diehl, T.; Vasquez, S.; Vassilev, P.M.; Teplow, D.B.; Selkoe, D.J. Protofibrillar Intermediates of Amyloid β-Protein Induce Acute Electrophysiological Changes and Progressive Neurotoxicity in Cortical Neurons. *J. Neurosci.* **1999**, *19*, 8876–8884. [CrossRef]

4. Chiti, F.; Dobson, C.M. Protein Misfolding, Functional Amyloid, and Human Disease. *Annu. Rev. Biochem.* **2006**, *75*, 333–366. [CrossRef] [PubMed]

5. Yankner, B.A.; Lu, T. Amyloid β-protein toxicity and the pathogenesis of Alzheimer disease. *J. Biol. Chem.* **2009**, *284*, 4755–4759. [CrossRef] [PubMed]

6. Pike, C.J.; Walencewicz-Wasserman, A.J.; Kosmoski, J.; Cribbs, D.H.; Glabe, C.G.; Cotman, C.W. Structure-Activity Analyses of β-Amyloid Peptides: Contributions of the β25-35 Region to Aggregation and Neurotoxicity. *J. Neurochem.* **2002**, *64*, 253–265. [CrossRef] [PubMed]

7. Harkany, T.; Hortobágyi, T.; Sasvári, M.; Kónya, C.; Penke, B.; Luiten, P.G.M.; Csaba, N. Neuroprotective approaches in experimental models of β-Amyloid neurotoxicity: Relevance to Alzheimer's disease. *Prog. Neuro Psychopharmacol. Biol. Psychiatry* **1999**, *23*, 963–1008. [CrossRef]

8. Harkany, T.; Ábrahám, I.; Kónya, C.; Nyakas, C.; Zarándi, M.; Penke, B.; Luiten, P.G.M. Mechanisms of ß-Amyloid Neurotoxicity: Perspectives of Pharmacotherapy. *Rev. Neurosci.* **2000**, *11*, 329–382. [CrossRef]

9. Markesbery, W.R.; Carney, J.M. Oxidative Alterations in Alzheimer's Disease. *Brain Pathol.* **2006**, *9*, 133–146. [CrossRef]

10. Butterfield, D.A.; Yatin, S.M.; Varadarajan, S.; Koppal, T. [48] Amyloid β-peptide-associated free radical oxidative stress, neurotoxicity, and Alzheimer's disease. In *Methods in Enzymology*; Academic Press: Cambridge, MA, USA, 1999; pp. 746–768.

11. Hensley, K.; Hall, N.; Subramaniam, R.; Cole, P.; Harris, M.; Aksenov, M.; Aksenova, M.; Gabbita, S.P.; Wu, J.F.; Carney, J.M.; et al. Brain Regional Correspondence Between Alzheimer's Disease Histopathology and Biomarkers of Protein Oxidation. *J. Neurochem.* **2002**, *65*, 2146–2156. [CrossRef]

12. Allan Butterfield, D. Amyloid β-peptide (1-42)-induced Oxidative Stress and Neurotoxicity: Implications for Neurodegeneration in Alzheimer's Disease Brain. A Review. *Free Radic. Res.* **2002**, *36*, 1307–1313. [CrossRef]

13. Cheignon, C.; Tomas, M.; Bonnefont-Rousselot, D.; Faller, P.; Hureau, C.; Collin, F. Oxidative stress and the amyloid beta peptide in Alzheimer's disease. *Redox Biol.* **2018**, *14*, 450–464. [CrossRef] [PubMed]

14. Smith, D.G.; Cappai, R.; Barnham, K.J. The redox chemistry of the Alzheimer's disease amyloid β peptide. *Biochim. Biophys. Acta Biomembr.* **2007**, *1768*, 1976–1990. [CrossRef] [PubMed]

15. Kanski, J.; Aksenova, M.; Butterfield, D.A. The hydrophobic environment of Met35 of Alzheimer's Aβ(1–42) is important for the neurotoxic and oxidative properties of the peptide. *Neurotox. Res.* **2002**, *4*, 219–223. [CrossRef] [PubMed]

16. Varadarajan, S.; Yatin, S.; Aksenova, M.; Butterfield, D.A. Review: Alzheimer's Amyloid β-Peptide-Associated Free Radical Oxidative Stress and Neurotoxicity. *J. Struct. Biol.* **2000**, *130*, 184–208. [CrossRef] [PubMed]

17. Enache, T.A.; Oliveira-Brett, A.M. Alzheimer's disease amyloid beta peptides in vitro electrochemical oxidation. *Bioelectrochemistry* **2017**. [CrossRef] [PubMed]

18. Vogt, W. Oxidation of methionyl residues in proteins: Tools, targets, and reversal. *Free Radic. Biol. Med.* **1995**, *18*, 93–105. [CrossRef]

19. Varadarajan, S.; Yatin, S.; Kanski, J.; Jahanshahi, F.; Butterfield, D.A. Methionine residue 35 is important in amyloid β-peptide-associated free radical oxidative stress. *Brain Res. Bull.* **1999**, *50*, 133–141. [CrossRef]

20. Yatin, S.M.; Varadarajan, S.; Link, C.D.; Butterfield, D.A. In vitro and in vivo oxidative stress associated with Alzheimer's amyloid ß-peptide (1–42). *Neurobiol. Aging* **1999**, *20*, 325–330.

21. Curtain, C.C.; Ali, F.; Volitakis, I.; Cherny, R.A.; Norton, R.S.; Beyreuther, K.; Barrow, C.J.; Masters, C.L.; Bush, A.I.; Barnham, K.J. Alzheimer's Disease Amyloid-β Binds Copper and Zinc to Generate an Allosterically Ordered Membrane-penetrating Structure Containing Superoxide Dismutase-like Subunits. *J. Biol. Chem.* **2001**, *276*, 20466–20473. [CrossRef]

22. Butterfield, D.A.; Boyd-Kimball, D. The critical role of methionine 35 in Alzheimer's amyloid β-peptide (1–42)-induced oxidative stress and neurotoxicity. *Biochim. Biophys. Acta Proteins Proteom.* **2005**, *1703*, 149–156. [CrossRef] [PubMed]

23. Gabbita, S.P.; Aksenov, M.Y.; Lovell, M.A.; Markesbery, W.R. Decrease in Peptide Methionine Sulfoxide Reductase in Alzheimer's Disease Brain. *J. Neurochem.* **2002**, *73*, 1660–1666. [CrossRef] [PubMed]

24. Butterfield, D.A.; Reed, T.; Newman, S.F.; Sultana, R. Roles of amyloid β-peptide-associated oxidative stress and brain protein modifications in the pathogenesis of Alzheimer's disease and mild cognitive impairment. *Free Radic. Biol. Med.* **2007**, *43*, 658–677. [CrossRef] [PubMed]

25. Varadarajan, S.; Kanski, J.; Aksenova, M.; Lauderback, C.; Butterfield, D.A. Different Mechanisms of Oxidative Stress and Neurotoxicity for Alzheimer's Aβ(1−42) and Aβ(25−35). *J. Am. Chem. Soc.* **2001**, *123*, 5625–5631. [CrossRef] [PubMed]

26. Bakhmutova-Albert, E.V.; Yao, H.; Denevan, D.E.; Richardson, D.E. Kinetics and Mechanism of Peroxymonocarbonate Formation. *Inorg. Chem.* **2010**, *49*, 11287–11296. [CrossRef]

27. Liochev, S.I.; Fridovich, I. Copper, Zinc Superoxide Dismutase and H_2O_2. *J. Biol. Chem.* **2002**, *277*, 34674–34678. [CrossRef]

28. Conrado, A.B.; D'Angelantonio, M.; Torreggiani, A.; Pecci, L.; Fontana, M. Reactivity of hypotaurine and cysteine sulfinic acid toward carbonate radical anion and nitrogen dioxide as explored by the peroxidase activity of Cu, Zn superoxide dismutase and by pulse radiolysis. *Free Radic. Res.* **2014**, *48*, 1300–1310. [CrossRef]

29. Perrin, D.; Koppenol, W.H. The Quantitative Oxidation of Methionine to Methionine Sulfoxide by Peroxynitrite. *Arch. Biochem. Biophys.* **2000**, *377*, 266–272. [CrossRef]

30. Spasojević, I.; Bogdanović Pristov, J.; Vujisić, L.; Spasić, M. The reaction of methionine with hydroxyl radical: Reactive intermediates and methanethiol production. *Amino Acids* **2012**, *42*, 2439–2445. [CrossRef]

31. Pryor, W.A.; Jin, X.; Squadrito, G.L. One- and two-electron oxidations of methionine by peroxynitrite. *Proc. Natl. Acad. Sci. USA* **1994**, *91*, 11173–11177. [CrossRef]

32. Yim, M.B.; Chock, P.B.; Stadtman, E.R. Copper, zinc superoxide dismutase catalyzes hydroxyl radical production from hydrogen peroxide. *Proc. Natl. Acad. Sci. USA* **1990**, *87*, 5006–5010. [CrossRef] [PubMed]

33. Stellato, F.; Fusco, Z.; Chiaraluce, R.; Consalvi, V.; Dinarelli, S.; Placidi, E.; Petrosino, M.; Rossi, G.C.; Minicozzi, V.; Morante, S. The effect of β-sheet breaker peptides on metal associated Amyloid-β peptide aggregation process. *Biophys. Chem.* **2017**, *229*, 110–114. [CrossRef]

34. Butterfield, D.A.; Boyd-Kimball, D. Amyloid β-Peptide(1-42) Contributes to the Oxidative Stress and Neurodegeneration Found in Alzheimer Disease Brain. *Brain Pathol.* **2006**, *14*, 426–432. [CrossRef] [PubMed]

35. Aliev, G. Editorial [Hot Topic: Oxidative Stress Induced-Metabolic Imbalance, Mitochondrial Failure, and Cellular Hypoperfusion as Primary Pathogenetic Factors for the Development of Alzheimer Disease Which Can Be Used as an Alternate and Successful Drug Treatment Strategy: Past, Present and Future (Guest Editor: Gjumrakch Aliev)]. *CNS Neurol. Disord. Drug Targets* **2011**, *10*, 147–148. [PubMed]

36. França, M.B.; Lima, K.C.; Eleutherio, E.C.A. Oxidative Stress and Amyloid Toxicity: Insights from Yeast. *J. Cell. Biochem.* **2017**, *118*, 1442–1452. [CrossRef]

37. Zhang, H.; Joseph, J.; Gurney, M.; Becker, D.; Kalyanaraman, B. Bicarbonate Enhances Peroxidase Activity of Cu, Zn-Superoxide Dismutase. *J. Biol. Chem.* **2002**, *277*, 1013–1020. [CrossRef] [PubMed]

38. Medinas, D.B.; Cerchiaro, G.; Trindade, D.F.; Augusto, O. The carbonate radical and related oxidants derived from bicarbonate buffer. *IUBMB Life* **2007**, *59*, 255–262. [CrossRef]

39. Medinas, D.B.; Toledo, J.C., Jr.; Cerchiaro, G.; Do-Amaral, A.T.; De-Rezende, L.; Malvezzi, A.; Augusto, O. Peroxymonocarbonate and Carbonate Radical Displace the Hydroxyl-like Oxidant in the Sod1 Peroxidase Activity under Physiological Conditions. *Chem. Res. Toxicol.* **2009**, *22*, 639–648. [CrossRef]

40. Trindade, D.F.; Cerchiaro, G.; Augusto, O. A Role for Peroxymonocarbonate in the Stimulation of Biothiol Peroxidation by the Bicarbonate/Carbon Dioxide Pair. *Chem. Res. Toxicol.* **2006**, *19*, 1475–1482. [CrossRef]

41. Petrat, F.; de Groot, H.; Rauen, U. Subcellular distribution of chelatable iron: A laser scanning microscopic study in isolated hepatocytes and liver endothelial cells. *Biochem. J.* **2001**, *356*, 61. [CrossRef]

42. Swaim, M.W.; Pizzo, S.V. Methionine Sulfoxide and the Oxidative Regulation of Plasma Proteinase Inhibitors. *J. Leukoc. Biol.* **1988**, *43*, 365–379. [CrossRef] [PubMed]

43. Brot, N.; Weissbach, H. Biochemistry and physiological role of methionine sulfoxide residues in proteins. *Arch. Biochem. Biophys.* **1983**, *223*, 271–281. [CrossRef]

44. Richardson, D.E.; Yao, H.; Frank, K.M.; Bennett, D.A. Equilibria, Kinetics, and Mechanism in the Bicarbonate Activation of Hydrogen Peroxide: Oxidation of Sulfides by Peroxymonocarbonate. *J. Am. Chem. Soc.* **2000**, *122*, 1729–1739. [CrossRef]

45. Richardson, D.E.; Regino, C.A.S.; Yao, H.; Johnson, J.V. Methionine oxidation by peroxymonocarbonate, a reactive oxygen species formed from CO_2/bicarbonate and hydrogen peroxide. *Free Radic. Biol. Med.* **2003**, *35*, 1538–1550. [CrossRef]

46. Liochev, S.I.; Fridovich, I. Copper, Zinc Superoxide Dismutase as a Univalent NO−Oxidoreductase and as a Dichlorofluorescin Peroxidase. *J. Biol. Chem.* **2001**, *276*, 35253–35257. [CrossRef]

47. Palmblad, M.; Westlind-Danielsson, A.; Bergquist, J. Oxidation of Methionine 35 Attenuates Formation of Amyloid β-Peptide 1–40 Oligomers. *J. Biol. Chem.* **2002**, *277*, 19506–19510. [CrossRef]

48. Hou, L.; Kang, I.; Marchant, R.E.; Zagorski, M.G. Methionine 35 Oxidation Reduces Fibril Assembly of the Amyloid Aβ-(1–42) Peptide of Alzheimer's Disease. *J. Biol. Chem.* **2002**, *277*, 40173–40176. [CrossRef]

49. Brown, A.M.; Lemkul, J.A.; Schaum, N.; Bevan, D.R. Simulations of monomeric amyloid β-peptide (1–40) with varying solution conditions and oxidation state of Met35: Implications for aggregation. *Arch. Biochem. Biophys.* **2014**, *545*, 44–52. [CrossRef] [PubMed]

50. Gu, M.; Viles, J.H. Methionine oxidation reduces lag-times for amyloid-β(1–40) fiber formation but generates highly fragmented fibers. *Biochim. Biophys. Acta Proteins Proteom.* **2016**, *1864*, 1260–1269. [CrossRef] [PubMed]

51. Ponzini, E.; De Palma, A.; Cerboni, L.; Natalello, A.; Rossi, R.; Moons, R.; Konijnenberg, A.; Narkiewicz, J.; Legname, G.; Sobott, F.; et al. Methionine oxidation in -synuclein inhibits its propensity for ordered secondary structure. *J. Biol. Chem.* **2019**, *294*, 5657–5665. [CrossRef] [PubMed]

52. Chen, S.; Hoffman, M.Z. Rate Constants for the Reaction of the Carbonate Radical with Compounds of Biochemical Interest in Neutral Aqueous Solution. *Radiat. Res.* **1973**, *56*, 40. [CrossRef]

53. Augusto, O.; Bonini, M.G.; Amanso, A.M.; Linares, E.; Santos, C.C.X.; De Menezes, S.L. Nitrogen dioxide and carbonate radical anion: Two emerging radicals in biology. *Free Radic. Biol. Med.* **2002**, *32*, 841–859. [CrossRef]

54. Huie, R.E.; Shoute, L.C.T.; Neta, P. Temperature dependence of the rate constants for reactions of the carbonate radical with organic and inorganic reductants. *Int. J. Chem. Kinet.* **1991**, *23*, 541–552. [CrossRef]

55. Yang, X.-H.; Huang, H.-C.; Chen, L.; Xu, W.; Jiang, Z.-F. Coordinating to Three Histidine Residues: Cu(II) Promotes Oligomeric and Fibrillar Amyloid-β Peptide to Precipitate in a Non-β Aggregation Manner. *J. Alzheimer's Dis.* **2009**, *18*, 799–810. [CrossRef] [PubMed]

56. Nair, N.G.; Perry, G.; Smith, M.A.; Reddy, V.P. NMR Studies of Zinc, Copper, and Iron Binding to Histidine, the Principal Metal Ion Complexing Site of Amyloid-β Peptide. *J. Alzheimer's Dis.* **2010**, *20*, 57–66. [CrossRef]

57. Barnham, K.J.; Bush, A.I. Metals in Alzheimer's and Parkinson's Diseases. *Curr. Opin. Chem. Biol.* **2008**, *12*, 222–228. [CrossRef]

58. Rauk, A.; Yu, D.; Taylor, J.; Shustov, G.V.; Block, D.A.; Armstrong, D.A. Effects of Structure on α C−H Bond Enthalpies of Amino Acid Residues: Relevance to H Transfers in Enzyme Mechanisms and in Protein Oxidation †. *Biochemistry* **1999**, *38*, 9089–9096. [CrossRef]

59. Schöneich, C.; Pogocki, D.; Hug, G.L.; Bobrowski, K. Free Radical Reactions of Methionine in Peptides: Mechanisms Relevant to β-Amyloid Oxidation and Alzheimer's Disease. *J. Am. Chem. Soc.* **2003**, *125*, 13700–13713. [CrossRef]

60. Hildebrandt, A.G.; Roots, I. Reduced nicotinamide adenine dinucleotide phosphate (NADPH)-dependent formation and breakdown of hydrogen peroxide during mixed function oxidation reactions in liver microsomes. *Arch. Biochem. Biophys.* **1975**, *171*, 385–397. [CrossRef]

61. Hirschberger, L.L.; de la Rosa, J.; Stipanuk, M.H. Determination of cysteinesulfinate, hypotaurine and taurine in physiological samples by reversed-phase high-performance liquid chromatography. *J. Chromatogr. B Biomed. Sci. Appl.* **1985**, *343*, 303–313. [CrossRef]

62. Perluigi, M.; Di Domenico, F.; Blarzino, C.; Foppoli, C.; Cini, C.; Giorgi, A.; Grillo, C.; De Marco, F.; Butterfield, D.A.; Schininà, M.E.; et al. Effects of UVB-induced oxidative stress on protein expression and specific protein oxidation in normal human epithelial keratinocytes: A proteomic approach. *Proteome Sci.* **2010**. [CrossRef] [PubMed]

63. Fontana, M.; Giovannitti, F.; Pecci, L. The protective effect of hypotaurine and cysteine sulphinic acid on peroxynitrite-mediated oxidative reactions. *Free Radic. Res.* **2008**, *42*, 320–330. [CrossRef] [PubMed]

64. Kanski, J.; Varadarajan, S.; Aksenova, M.; Butterfield, D.A. Role of glycine-33 and methionine-35 in Alzheimer's amyloid β-peptide 1–42-associated oxidative stress and neurotoxicity. *Biochim. Biophys. Acta Mol. Basis Dis.* **2002**, *1586*, 190–198. [CrossRef]

65. Cricenti, A.; Colonna, S.; Girasole, M.; Gori, P.; Ronci, F.; Longo, G.; Dinarelli, S.; Luce, M.; Rinaldi, M.; Ortenzi, M. Scanning probe microscopy in material science and biology. *J. Phys. D Appl. Phys.* **2011**, *44*, 464008. [CrossRef]

66. Giles, G.I.; Jacob, C. Reactive Sulfur Species: An Emerging Concept in Oxidative Stress. *Biol. Chem.* **2002**, *383*, 375–388. [CrossRef]

67. Jacob, C. A scent of therapy: Pharmacological implications of natural products containing redox-active sulfur atoms. *Nat. Prod. Rep.* **2006**, *23*, 851. [CrossRef]

Sample Availability: Samples of the compounds are available from the authors.